

Improved prognostic value of recurrence for atrial fibrillation patients after cryoablation by non-linear survival models

Jing Li¹, Xuewen Liao², Lin Chen², Zhi-Ping Yang², Jian-Quan Chen², Jian-Cheng Zhang², Yazhou Lin², and Xiaoping Chen³

¹Fujian Normal University School of Mathematics and Statistics

²Fujian Provincial Hospital

³Fujian University of Technology

September 20, 2023

Abstract

Background: Atrial fibrillation (AF) is a common cardiac arrhythmia that affects millions of people worldwide. We aim to investigate how to improve prognostic value of recurrence for atrial fibrillation patients after cryoablation by non-linear survival models. **Methods:** In this study, we retrospectively reviewed data from 1023 patients who underwent cryoablation surgery for AF at Fujian Provincial Hospital (FPH). We generated radiomics signatures (RSI) and a clinical signature (CLI) using a non-linear survival model by repeated 10-fold cross-validation. The comprehensive risk score (TCRS) was obtained by linearly weighting the multivariate Cox proportional risk model. **Results:** The combination of RSI and CLI indicators had a significantly higher area under the curve (AUC) in the ROC curve of the training set (AUC=0.955) compared to the AUC of a single indicator CLI (AUC=0.862). The TCRS showed better prognostic performance compared to the traditional Lasso-Cox models, with AUC of 0.955 vs 0.664. The accuracy of the model was further confirmed by the C-indices of RSI (C-index: 0.8894; 95%CI: 0.8166-0.9621), CLI (C-index: 0.8431; 95%CI: 0.7466-0.9395), and TCRS (C-index: 0.9072; 95%CI: 0.8281-0.9864) in validation set 2. **Conclusions:** Under a nonlinear survival model, TCRS which combines RSI and CLI indicators has potential as a promising prognostic tool for post-cryoablation AF patients.

Improved prognostic value of recurrence for atrial fibrillation patients after cryoablation by non-linear survival models

Jing Li^{1, +}, Xuewen Liao^{2, +}, Lin Chen², Zhiping Yang², Jianquan Chen², Jiancheng Zhang², Yazhou Lin², Xiaoping Chen^{3, *}

Abstract

Background: Atrial fibrillation (AF) is a common cardiac arrhythmia that affects millions of people worldwide. We aim to investigate how to improve prognostic value of recurrence for atrial fibrillation patients after cryoablation by non-linear survival models.

Methods: In this study, we retrospectively reviewed data from 1023 patients who underwent cryoablation surgery for AF at Fujian Provincial Hospital (FPH). We generated radiomics signatures (RSI) and a clinical signature (CLI) using a non-linear survival model by repeated 10-fold cross-validation. The comprehensive risk score (TCRS) was obtained by linearly weighting the multivariate Cox proportional risk model.

Results: The combination of RSI and CLI indicators had a significantly higher area under the curve (AUC) in the ROC curve of the training set (AUC=0.955) compared to the AUC of a single indicator CLI (AUC=0.862). The TCRS showed better prognostic performance compared to the traditional Lasso-Cox models, with AUC of 0.955 vs 0.664. The accuracy of the model was further confirmed by the C-indices

of RSI (C-index: 0.8894; 95%CI: 0.8166-0.9621), CLI (C-index: 0.8431; 95%CI: 0.7466-0.9395), and TCRS (C-index: 0.9072; 95%CI: 0.8281-0.9864) in validation set 2.

Conclusions: Under a nonlinear survival model, TCRS which combines RSI and CLI indicators has potential as a promising prognostic tool for post-cryoablation AF patients.

Keywords

Atrial fibrillation, Cryoablation, Prognosis, Non-linear survival models

¹ College of Mathematics and Statistics & FJKLMAA, Fujian Normal University, Fuzhou, China

² Shengli Clinical Medical College of Fujian Medical University, Department of cardiology, Fujian Provincial Hospital, Fuzhou, China

³ School of Computer Science and Mathematics, Fujian University of Technology, Fuzhou, China

* Corresponding author at: No3 Xueyuan Road, University Town, Minhou, Fuzhou City, Fujian Province, 350118, China

E-mail address: exp155@163.com.

+ These authors share first authorship.

Background

Atrial fibrillation (AF) is a common clinical arrhythmia, with a high incidence in the population, which can cause chest tightness, palpitations, shortness of breath and other uncomfortable symptoms during the attack, and can also lead to serious complications such as stroke, peripheral artery embolism, cardiac insufficiency, and sudden cardiac death[1, 2]. In recent years, under the background of the rapid development of medical science and technology, the second-generation cryoballoon ablation (CBA) has been gradually applied to the clinic, and its safety and effectiveness in the treatment of atrial fibrillation are the contents of great clinical concern[3]. In a single-center study with a one-year follow-up that assessed clinical outcomes using CB2, the recurrence rate was about 80% for paroxysmal atrial fibrillation (PAF) and 60 to 70 percent for persistent atrial fibrillation (SAF)[4-8]. This study reported patients with AF underwent a second-generation cryoballoon ablation (CBA) from Fujian Provincial Hospital (FPH). And the AF pattern include Paroxysmal, Persistent, and Long-standing persistent.

Many studies have determined prognostic factors based on traditional least absolute shrinkage and selection operator regression (Lasso) with the multivariable Cox survival models[9], and other scholars have used nomograms to construct predictive models[10]. Some scholars have used by machine learning which is a field of computer science that uses computer algorithms to identify patterns in multivariable datasets and can be used to predict[11], but most of them only build risk scoring models for data for one machine learning method[12-14]. Based on the Cox proportional hazards model, this study combines machine learning methods to train nonlinear features and calculate their linear combinations to estimate the risk function. That is, the nonlinear survival model[15]. The Faraggi-Simon method is a feed-forward neural network that provides the basis for nonlinear proportional hazard models. In our study, we evaluated the benefits of combining the multivariable Cox survival models with some machine learning algorithms. The prediction effect is measured by the AUC value under the ROC curve, and radioactivity signature and clinical indicators were constructed to explore and analyze the recurrence rate of patients after cryoablation surgery.

Methods

Data source

The data of 1023 patients who had been treated by cryoablation at Fujian Provincial Hospital (FPH) between April 2016 and November 2019 were reviewed retrospectively. Patients were assessed at the 3rd, 6th, 12th months in the first year post-ablation and at 6-month intervals thereafter with a 12-lead ECG and a 24-hour Holter ECG. Written informed consents for tissue collection were obtained from all patients prior to inclusion.

The random forest method was adopted for interpolation when the clinicopathological data were partially missing, and the missing rate of the data was less than 10%. Patients were randomly divided into training set and validation set according to the ratio of 7:2:1, of which 716 patients were in the training set, 204 patients were in the validation set 1 and 103 patients in the validation set 2. The primary clinical endpoint was disease-free survival (DFS), which is from the date of surgery to the date of recurrence, metastasis, or last follow-up.

Pre-procedural management and variable description

Perioperative anticoagulation management throughout the whole procedure according to current AF consensus. Antiarrhythmic drugs were discontinued five half-lives before the CBA procedure. All patients underwent transthoracic echocardiography (TTE) to assess the left atrial diameter, ejection fraction (EF), and standard clinical 12-lead electrocardiography (ECG) recordings with sinus rhythm to measure P-wave duration and amplitude. Transesophageal echocardiographic (TEE) was used to exclude LA or left atrial appendage thrombus prior to the CBA procedure. All assessments were performed by trained technicians, who were blinded to the clinical characteristics of the participants. Computed tomography angiography for 3D reconstruction of LA/PVs (pulmonary veins) directly illustrates the number, branches, morphology, and anatomic variants of the PVs. It also can screen the thrombus of LA and the left atrial appendage. Left atrial area (Laa) and Vertebral area (Va) were simultaneously measured by two radiologists, blinded to all patient data.

Based on the variables measured by radiologists, we extracted radiological features (RSI), including 13 features. The continuous variables are Left atrial area (Laa), Vertebral area (Va), Laa/Va, LA anteroposterior (Ap), LA transverse (Trans), Left superior pulmonary vein (LSPV), Left lower pulmonary vein (Llpv), Right superior pulmonary vein (RSPV) and Right lower pulmonary vein (Rlpv). The dichotomous variables are Rmpv (Yes or No) \ Lmpv (Yes or No) \ Trunk (Yes or No) and anatomy anatomical abnormalities of pulmonary veins (Yes or No). Furthermore, the clinical patients data obtained included 32 variables. Age, gender, AF History, left atrium diameter (LA), left ventricle diameter (LV), ejection fraction (EF), body mass index (BMI), NTpro-BNP, creatinine clearance (Ccr), Uric acid (UA), Personal Activity Intelligence (PAI), Intra Aortic Balloon (IAB), Ptfv1, atrial fibrillation (AF), CHA₂DS₂-VASc, HAS-BLED scores, New York Heart Association Class IV, Stoke, TAI, coronary artery disease (CAD), PCI, hypertension (HP), DM, HCM, lipid metabolism abnormalities (Lipid), PreAAD, Smoke, Drink, PM, Ablationtype, antiarrhythmic drugs(AAD. Discharged) and Pre.Amiodarone were also taken into consideration.

Statistical analysis

In baseline characteristics, continuous variables with normal distribution were expressed as mean \pm standard deviation (SD) or median if not normally distributed which were using the t-test, and categorical variables were analyzed using chi-square test. All tests were two-sided; $P < 0.05$ was considered significant.

Based on the Cox proportional-hazards model, we combined with the nonlinear regression model which contains a variety of machine learning to obtain a nonlinear survival model. In the non-linear part of building RSI and CLI, we used a variety of machine learning methods to compare, such as Gradient Boosting, Support Vector Machine, Random Forest, K-Nearest Neighbor, and Neural Network. The best cut-off for dividing patients into low-risk and high-risk groups was picked using X-tile plots based on the association with patients' survival time. The Kaplan-Meier curve analysis and the log-rank test was used to estimate the cumulative survival curves of recurrence during the follow-up period. The prognostic effect of the risk score model was observed by using the receiver operating characteristic (ROC) curve with area under curve (AUC) value and Harrell's concordance index (C-index). All analyses were conducted using R (version 4.2.2).

Results

Baseline characteristics

A total of 1023 postoperative patients were enrolled, with 716 patients in the training set, 204 patients were in the validation set 1 and 103 patients in the validation set 2. The median follow-up time was 13 months

(ranging from 3 to 48 months). During the follow-up period, 179 patients (17.5%) experienced relapse, 37 patients (20.7%) underwent repeated ablation, and 7 patients (0.7%) died of non-cardiac causes. Significant differences in radiomics and clinical features were shown in patients with different types of atrial fibrillation (Table 1; Supplemental Table 1).

Table 1 Baseline Characteristics.

Characteristics	All patients (n=1023)	Paroxysmal AF (n = 641)	Persistent AF (n = 382)	P-value
Radiomics features	Radiomics features	Radiomics features	Radiomics features	Radiomics features
Laa, cm ²	25.5 ± 6.28	23.82 ± 5.54	28.32 ± 6.46	< 0.001
Ap, cm	4.1 ± 0.88	3.92 ± 0.83	4.4 ± 0.87	< 0.001
Trans, cm	7.31 ± 1.01	7.09 ± 0.91	7.68 ± 1.06	< 0.001
LSPV, cm	10.2 (8.5, 11.9)	10.3 (8.6, 12)	10 (8.43, 11.6)	0.263
RSPV, cm	10.8 (9.2, 12.7)	11 (9.3, 12.8)	10.6 (9.1, 12.55)	0.135
Clinical features	Clinical features	Clinical features	Clinical features	Clinical features
Age, y	61.33 ± 10.03	62.04 ± 9.78	60.13 ± 10.34	0.004
Gender, n (%)				0.003
Male	674 (66)	400 (62)	274 (72)	
Female	349 (34)	241 (38)	108 (28)	
AF History, m	2 (0.5, 5)	2 (0.58, 5)	2 (0.5, 5)	0.483
LA, cm	3.92 ± 0.64	3.71 ± 0.57	4.26 ± 0.6	< 0.001
LV, cm	4.63 ± 0.51	4.61 ± 0.51	4.67 ± 0.5	0.062
EF, %	60.04 ± 5.39	60.55 ± 5.25	59.18 ± 5.53	< 0.001
BMI, kg/m ²	24.3 ± 3.16	23.99 ± 3.14	24.82 ± 3.12	< 0.001
NT-ProBNP, pg/ml	320.4 (128.39, 686.83)	211.3 (90.98, 423.87)	606.3 (326.15, 899.75)	< 0.001
Ccr, %	90.46 (74.06, 108.53)	89.47 (72.73, 108.53)	92.01 (77.05, 108.53)	0.143
UA, Mmol/L	364.35 ± 93.95	353.01 ± 93.89	383.38 ± 91.05	< 0.001
PAI, n (%)				< 0.001
No	341 (33)	242 (38)	99 (26)	
Yes	682 (67)	399 (62)	283 (74)	
NYHA, n (%)				< 0.001
No	875 (86)	568 (89)	307 (80)	
Yes	148 (14)	73 (11)	75 (20)	
PreAAD, n (%)				0.004
No	502 (49)	340 (53)	162 (42)	
Class I	268 (26)	155 (24)	113 (30)	
Class II	154 (15)	83 (13)	71 (19)	
Class III	99 (10)	63 (10)	36 (9)	
Ablationtype, n (%)				< 0.001
PVI	851 (83)	641 (100)	210 (55)	
+PV antrum	85 (8)	0 (0)	85 (22)	
+Roof linear	87 (9)	0 (0)	87 (23)	
AAD.Discharged, n (%)				< 0.001
No	173 (17)	139 (22)	34 (9)	
Class I	330 (32)	114 (18)	216 (57)	

Class II	332 (32)	286 (45)	46 (12)	
Class III	62 (6)	47 (7)	15 (4)	
Class IV	126 (12)	55 (9)	71 (19)	
Pre.Amiodarone, n (%)				< 0.001
No	834 (82)	569 (89)	265 (69)	
Yes	189 (18)	72 (11)	117 (31)	
Data are presented as mean±SD or median (quartile).				
AF atrial fibrillation; LA, left atrium diameter; LV, left ventricle diameter;EF, ejection fraction; BMI, body mass index; Ccr, creatinine clearance; UA, Uric acid; NYHA, New York Heart Association Class IV; Variables associated with antiarrhythmic drug status: PreAAD, AAD.Discharged.	AF atrial fibrillation; LA, left atrium diameter; LV, left ventricle diameter;EF, ejection fraction; BMI, body mass index; Ccr, creatinine clearance; UA, Uric acid; NYHA, New York Heart Association Class IV; Variables associated with antiarrhythmic drug status: PreAAD, AAD.Discharged.	AF atrial fibrillation; LA, left atrium diameter; LV, left ventricle diameter;EF, ejection fraction; BMI, body mass index; Ccr, creatinine clearance; UA, Uric acid; NYHA, New York Heart Association Class IV; Variables associated with antiarrhythmic drug status: PreAAD, AAD.Discharged.	AF atrial fibrillation; LA, left atrium diameter; LV, left ventricle diameter;EF, ejection fraction; BMI, body mass index; Ccr, creatinine clearance; UA, Uric acid; NYHA, New York Heart Association Class IV; Variables associated with antiarrhythmic drug status: PreAAD, AAD.Discharged.	AF atrial fibrillation; LA, left atrium diameter; LV, left ventricle diameter;EF, ejection fraction; BMI, body mass index; Ccr, creatinine clearance; UA, Uric acid; NYHA, New York Heart Association Class IV; Variables associated with antiarrhythmic drug status: PreAAD, AAD.Discharged.

Feature selection and radiomics signature building

The radiomics signature (RSI) included a total of 13 categories, such as Laa, Va and Trans (refer to section 2.2 for details). Moving on to feature selection and radiomics signature building, we employed six machine learning algorithms, including Gradient Boosting, Support Vector Machine, AdaBoost, Random Forest, K-Nearest Neighbor, and Neural Network, to build a radiomics signatures index (RSI) that could independently predict disease-free survival (DFS) based on the phenotypic characteristics of CT and PET images. The nonlinear survival model was utilized to generate a new feature by predicting survival outcomes via multiple machine learning.

Subsequently, repeated 10-fold cross-validation was used to evaluate the superiority of the trained model, and the Random Forest algorithm was found to obtain a higher AUC (Table 2). The results showed that the AUC value obtained by the random forest model was 0.8587 (95% CI: 0.8421-0.8753). Notably, the prediction accuracy of the model was 0.8529 (95% CI: 0.7968-0.8985). The importance indicators and sorting results of features in the Random Forest model were illustrated (Fig. 1), and the Random Forest algorithm was employed to extract the corresponding radiomics signatures index (RSI) from the imaging data of each patient.

Table 2 Machine learning outcomes of RSI.

Model	AUC(95%CI)	Precision	Recall	F
Gradient Boosting	0.8478[0.8291,0.8666]	0.8269	0.9738	0.8943
Support Vector Machine	0.8182[0.7996,0.8368]	0.8255	1.0000	0.9044
AdaBoost	0.8551[0.8387,0.8716]	0.8290	0.9924	0.9033
Random Forest	0.8587[0.8421,0.8753]	0.8337	0.9746	0.8986
K-Nearest Neighbor	0.7963[0.7766,0.816]	0.8259	0.9992	0.9043
Neural Network	0.8545[0.8388,0.8703]	0.8278	0.9873	0.9003

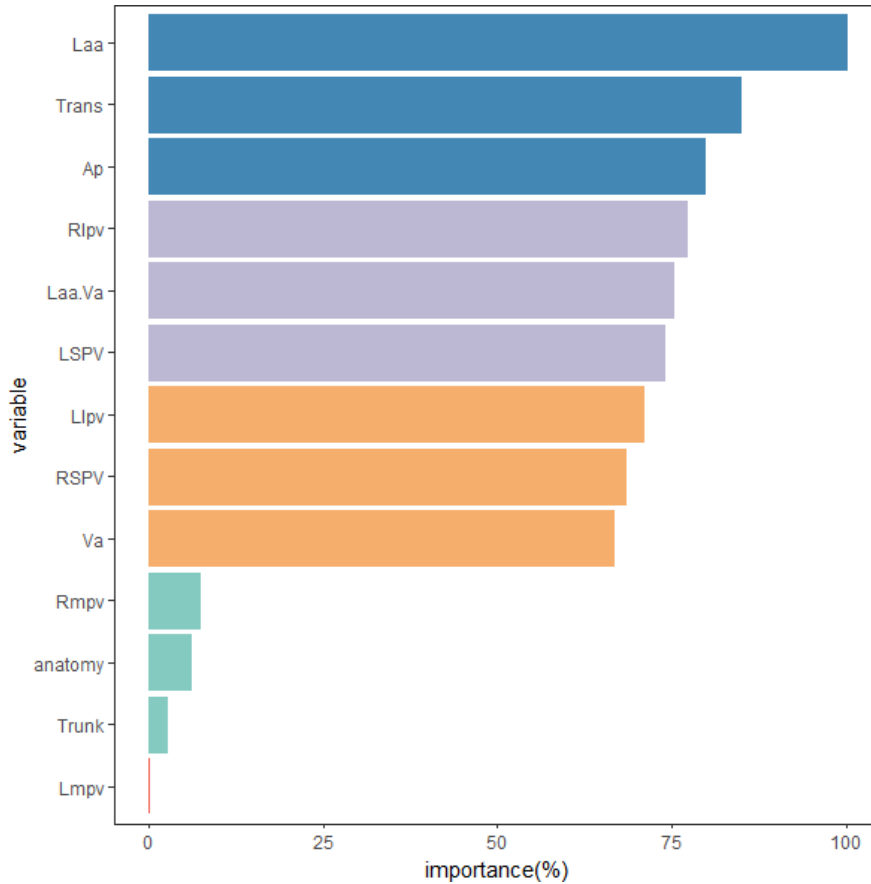


Fig. 1 Ranking of variable importance of RSI in Random Forest model.

Feature selection and clinical signature development

The clinical feature variables included a total of 32 categories (refer to section 2.2 for details). To construct clinical features (CLI), we followed the same method as in the previous section. Firstly, six machine learning algorithms, including Gradient Boosting, Support Vector Machine, AdaBoost, Random Forest, K-Nearest Neighbor, and Neural Network, were employed, and the results indicated that the Support Vector Machine model was better prediction results (Table 3).

The Support Vector Machine model boasted a prediction accuracy of 0.8627 (95% CI: 0.8078-0.9068). To extract the corresponding CLI, the Support Vector Machine algorithm was implemented on the clinical data of each patient. The importance variables and ranking results of features in the Support Vector Machine model were revealed in Fig. 2. Subsequently, the Support Vector Machine algorithm was utilized to extract the corresponding CLI from the clinical data of each patient.

Table 3 Machine learning outcomes of CLI.

Model	AUC(95%CI)	Precision	Recall	F
Gradient Boosting	0.852[0.8161,0.8879]	0.8253	0.8253	0.9039
Support Vector Machine	0.8526[0.8185,0.8866]	0.8253	0.8253	0.9040
AdaBoost	0.8522[0.8212,0.8832]	0.8271	0.8271	0.9050
Random Forest	0.8522[0.8114,0.893]	0.8253	0.8253	0.9039
K-Nearest Neighbor	0.8126[0.7634,0.8619]	0.8254	0.8254	0.9044
Neural Network	0.8472[0.7954,0.8989]	0.8383	0.8383	0.8447

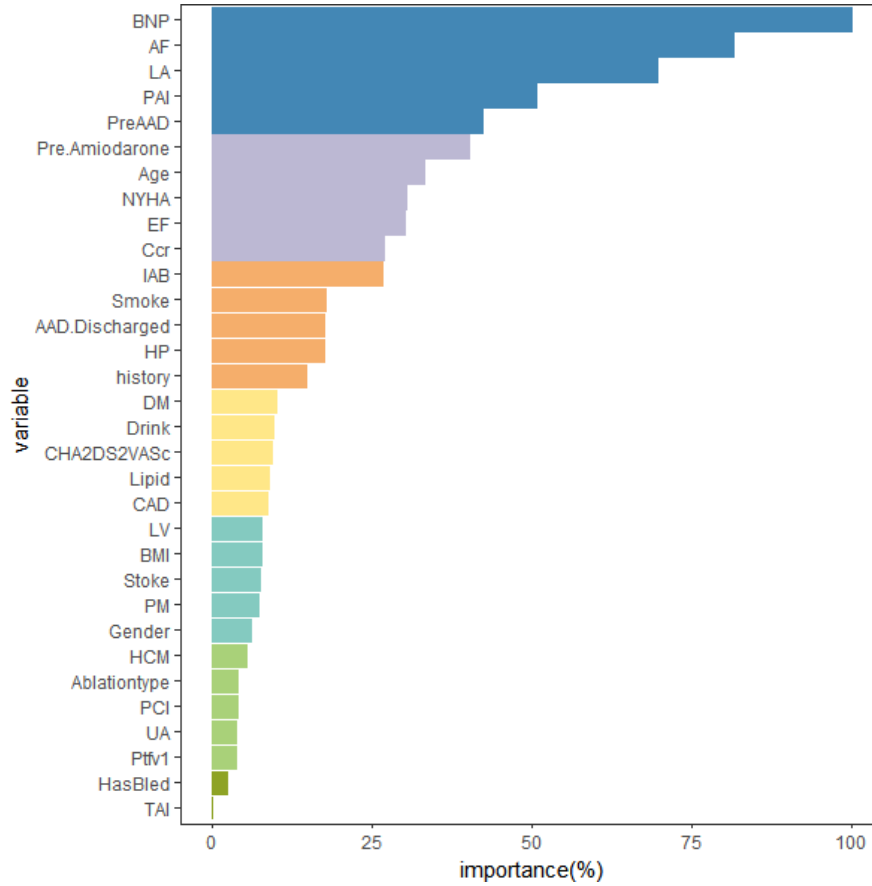


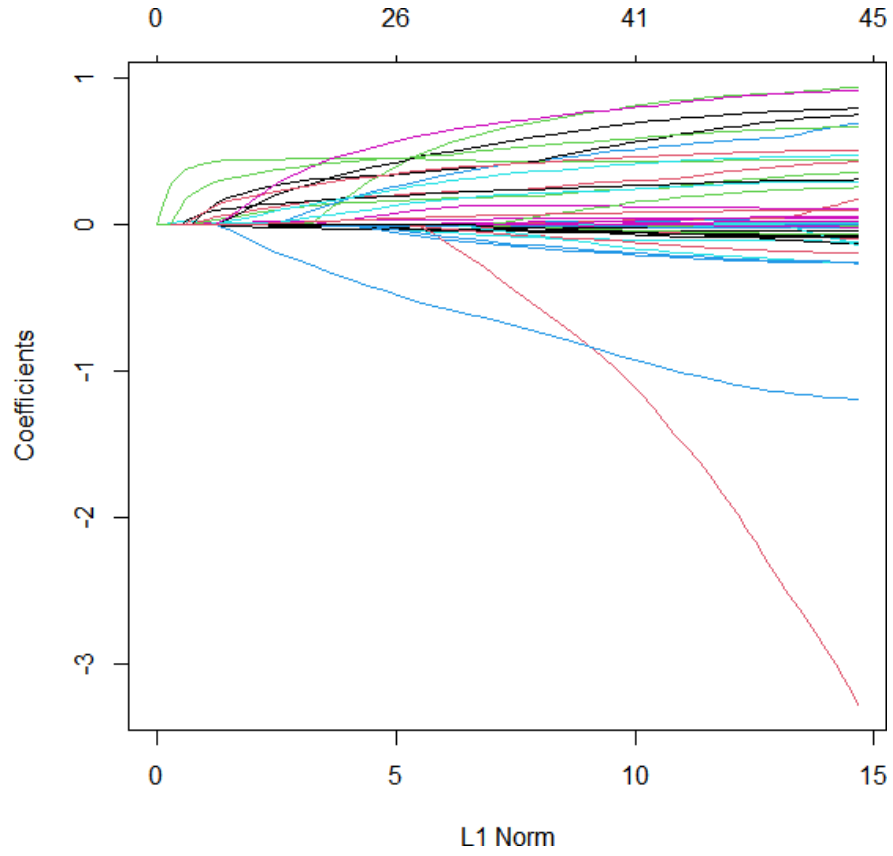
Figure 2. Ranking of variable importance of CLI in Support Vector Machine model.

Traditional Lasso Cox Models Building

To select the most useful prognostic combination of features, we employed the least absolute shrinkage and selection operator (LASSO) Cox regression method. In the training cohort of the whole dataset, we reduced 45 features to 4 prognostic markers (Laa, IAB, AF, and Pre.Amiodarone) with the LASSO Cox regression model, including non-zero coefficient features in the regression model (Fig. 3). Furthermore, through multivariate Cox stepwise regression, we filtered out four significant features (Table 4) and the formula for risk scores of final individual was derived:

We calculated RiskScore for each patient by computing a linear combination of the selected features, weighted

by their respective coefficients. Both features selection and risk signature construction were performed in the training set.



45 45 44 43 43 41 39 32 26 20 10 4 2 1

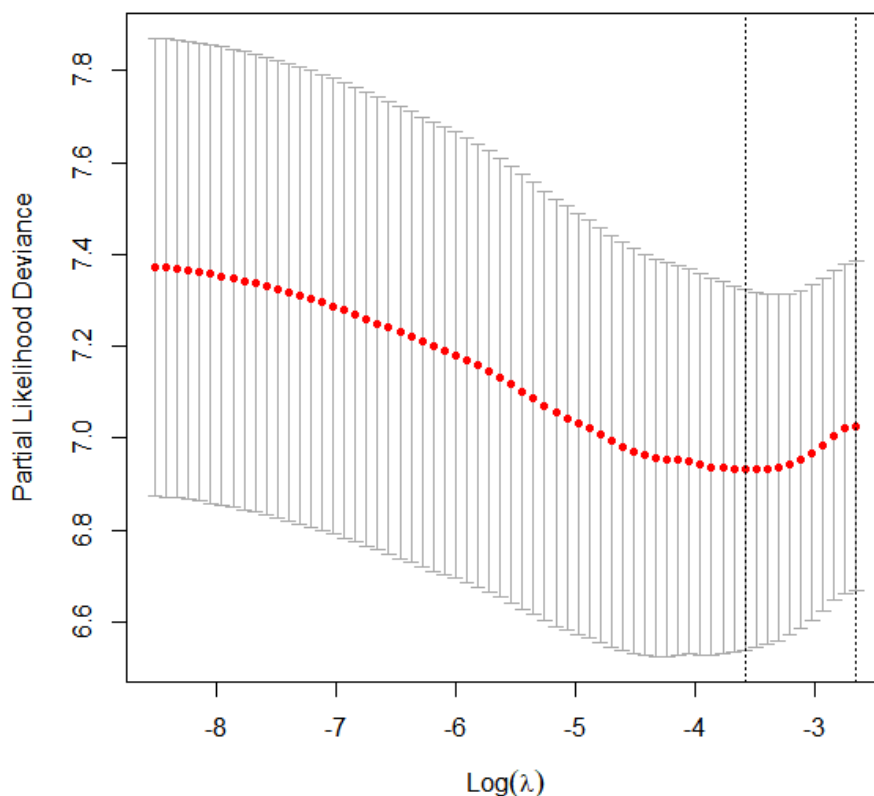


Fig. 3 Feature selection using LASSO regression model(A). Tuning parameter selection by 10-fold cross-validation via minimum criteria. Partial likelihood deviance was plotted versus $\log(\lambda)$ (B). Coefficient profile of characteristics associated with recurrence of patients. Vertical line is shown at the optimal value with four nonzero coefficients.

Table 4 The multivariate Cox analysis of RiskScore by Lasso model.

Characteristics	Coef	Hazard Ratio (HR)	95%CI	P-value
Laa	0.03308	1.03363	[1.004,1.064]	0.0261*
IAB	0.23914	1.27015	[1.014,1.591]	0.0372*
AF	0.58349	1.79229	[1.204,2.669]	0.0041*
Pre.Amiodarone	0.51319	1.67061	[1.104,2.528]	0.0151*
Statistically significant.	*Statistically significant.	*Statistically significant.	*Statistically significant.	*Statistically significant.

Predictive performance of the composite risk score

Based on the risk scores of radiological and clinical features constructed in the first two sections, we combined them through a Cox proportional hazard risk model to form the final postoperative patient risk score model. The results of multivariate Cox regression were shown in Table 5, and the ROC effect plot was shown in Fig. 4. We compared the traditional Lasso Cox model with the nonlinear survival model, and the results demonstrate that the nonlinear survival model provided much better indicators than Lasso Cox (Fig. 4), with an AUC ratio of 0.955 vs 0.664. Thus, we selected the indicator TCRS, which was constructed by the nonlinear survival model.

Additionally, the results of Harrell’s concordance index (Table 6) supported this. To determine the predictive effect of the nonlinear survival model, we compared the error between its predicted value and the true value by plotting calibration curves (Fig. 5). Using this result, we classified patients in the discovery cohort into low-risk and high-risk groups. In all sets, the high and low-risk groups we divided using the X-tile were always significant, with a P-value of less than 0.05. As the survival time increased, the survival rate of patients classified as high risk decreased significantly, while the survival rate of low-risk patients remained at a high level. The P-value of the log-rank test was less than 0.001 (Fig. 6). Finally, forestplot was drawn by combining some important indicators and TCRS variables with some machine learning to visually show the correlation between related variables and recurrence in patients with postoperative atrial fibrillation (Fig. 7).

Table 5 The multivariate Cox analysis of the composite risk score (TCRS).

Characteristics	Hazard Ratio (HR)	95%CI	P-value
RSI	570.0065	[266.155, 1220.7]	< 0.001
CLI	56.2765	[9.783, 323.7]	< 0.001

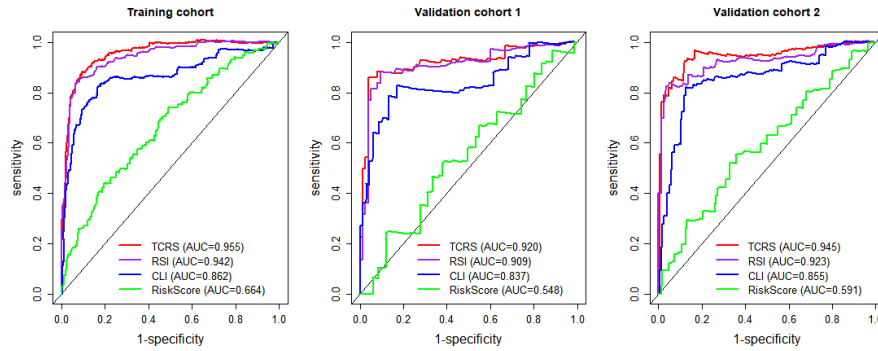


Fig. 4 ROC curve analysis of the composite riskscore (TCRS), radiomics signature (RSI), clinical index (CLI) and Risk-Score (Lasso-Cox) in training cohort (A), validation cohort 1 (B) and validation cohort 2 (C).

Table 6 The C-index of the risk models.

	Index	C-index	SE	95%CI	P-value
Whole cohort	RSI	0.9203	0.0099	[0.9008,0.9397]	< 0.001
	CLI	0.8377	0.0191	[0.8002,0.8752]	< 0.001
	TCRS	0.9334	0.0080	[0.9176,0.9491]	< 0.001
Training cohort	RSI	0.9291	0.0098	[0.9098,0.9483]	< 0.001
	CLI	0.8377	0.0236	[0.7914,0.8839]	< 0.001
	TCRS	0.9371	0.0077	[0.9221,0.9521]	< 0.001
Validation cohort 1	RSI	0.9125	0.0270	[0.8596,0.9653]	< 0.001
	CLI	0.8479	0.0420	[0.7656,0.9303]	< 0.001
	TCRS	0.9454	0.0120	[0.9219,0.9689]	< 0.001
Validation cohort 2	RSI	0.8894	0.0371	[0.8166,0.9621]	< 0.001
	CLI	0.8431	0.0492	[0.7466,0.9395]	< 0.001
	TCRS	0.9072	0.0404	[0.8281,0.9864]	< 0.001

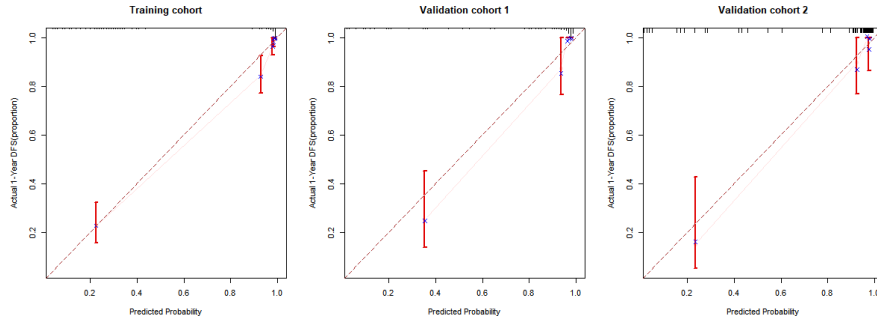


Fig. 5 Calibration curves of the non-linear survival model to predict DFS rate in training cohort in training cohort (A), validation cohort 1 (B) and validation cohort 2 (C).

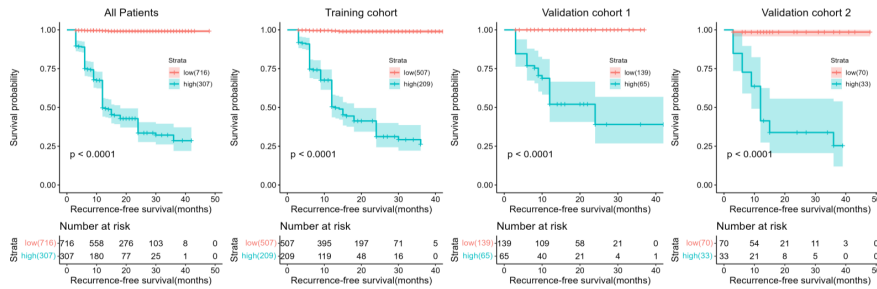


Fig. 6 Comparison of recurrence-free survival (DFS) in low-risk vs. high-risk patients stratified by Risk Score in all patients (A), training cohort (B), validation cohort 1 (C) and validation cohort 2 (D).

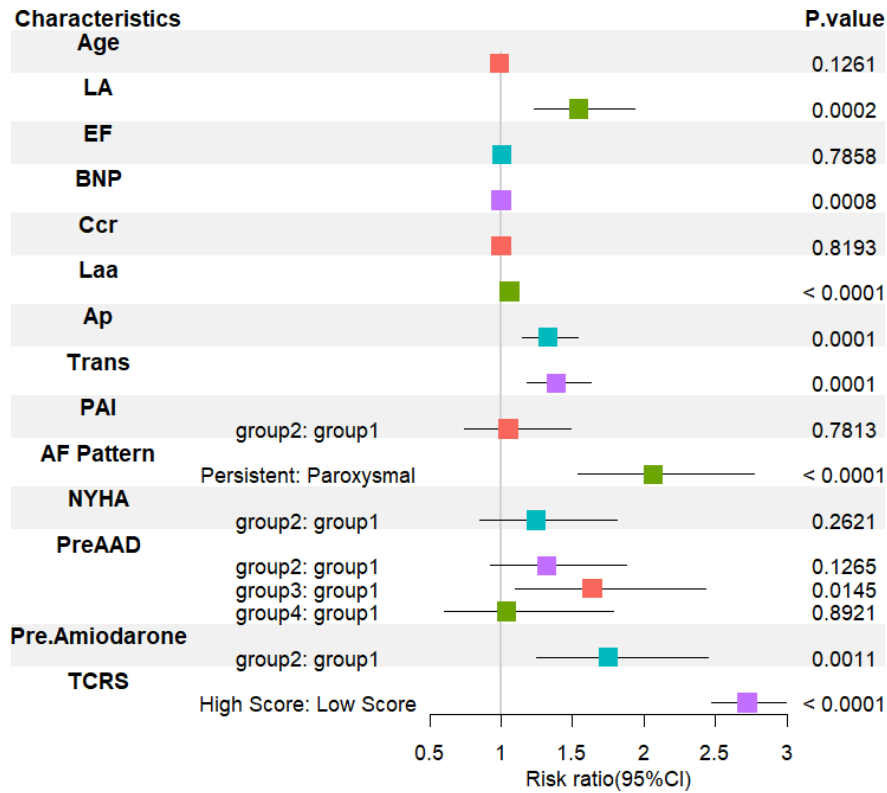


Fig. 7 Forest plot of important variables

Discussion

Atrial fibrillation is the most common sustained arrhythmia that increases with age and presents with a wide spectrum of symptoms and severity, including reentry theory and focal agitation[17,18]. Despite shorter ablation times, faster balloon cooling, and longer thawing times, ablation of atrial fibrillation with a second-generation cryoballoon is associated with higher success rates of pulmonary venous dissociation, acute and long-term PV isolation rates are high, AE rates are similar, and atrial fibrillation is absent[19]. Therefore, the data we collected and collated were all studies and analyses of AF patients after cryoablation.

In this study, prognostic variables were not simply analyzed by clinical index (CLI); imaging data was used to construct radioactivity index (RSI). With the joint action of clinical and radioactivity indicators, the C-index and ROC curve results of the formed risk score model showed a significant improvement in the prediction effect on the whole set, training set, validation set 1, or validation set 2. Meyre et al. (2019)[20] performed Cox regression analysis adjusted for risk factors for routine admission using clinical data to calculate the risk ratio (HR) and obtained a C-statistic of 0.64 (95% CI: 0.61-0.66). Similarly, Peng et al. (2019)[21] constructed radiomic features based on features extracted from PET and CT images in the training set to predict disease-free survival (DFS). To this end, the radioactivity indexes (RSI) of AF patients after cryoablation were integrated into this paper, and the original clinical indicators (CLI) were combined to form the comprehensive risk score (TCRS). From an effects standpoint, the combination of RSI and CLI indicators showed a significant increase compared to the AUC and C-index of a single indicator. In the ROC curve of the training set, the AUC of RSI was 0.942 and the AUC of CLI was 0.862, but the AUC of TCRS obtained by linearly weighting the two indicators was 0.955. Similarly, in the validation set 1, the TCRS index formed by TCRS showed superior prognostic performance. In order to improve the accuracy of the model, a second validation set was set up to witness the TCRS constructed from the nonlinear survival model. The results of the C-index also confirm the accuracy of the model, such as RSI (C-index: 0.8894;

95%CI: 0.8166-0.9621), CLI (C-index: 0.8431; 95%CI: 0.7466-0.9395), and TCRS (C-index: 0.9072; 95%CI: 0.8281-0.9864) in validation set 2.

Researchers have traditionally used Lasso Cox analysis to perform survival analyses for various diseases. Bieging et al. (2018)[22] selected only shape parameters using the Lasso method and factor analysis, adding them to a Cox regression model that included multiple clinical parameters and LA fibrosis (C-index: 0.68-0.72). Other scholars have used the nomogram method to analyze the postoperative prognosis of patients with AF. Zhou et al. (2021)[23] explored the risk factors for recurrence of atrial fibrillation (AF) in patients after radio frequency ablation and constructed a targeted nomogram prediction model (AUC=0.852). Dong et al. (2022)[24] used the least absolute shrinkage and selection operator regression for variable screening and a multi-variable Cox survival model for nomogram development, obtaining an AUC of between 0.855 and 0.863 in the development and validation cohorts. Our study combines the nonlinear part of machine learning and the linear part of the Cox model to obtain a nonlinear proportional risk survival model, enabling the construction of the risk score of AF patients to divide them into high- and low-risk groups. First, from the perspective of ROC curve, TCRS constructed from non-linear survival models had better prognosis whether in the training set (AUC: 0.955 vs 0.664), validation set 1 (AUC: 0.920 vs 0.548) or validation set 2 (AUC: 0.945 vs 0.591). The closer the AUC is to 1, the better the prediction. Second, the results were more credible through the auxiliary verification of C-index, such as RSI (C-index: 0.9125; 95%CI: 0.8596-0.9653), CLI (C-index: 0.8479; 95%CI: 0.7656-0.9303) and TCRS (C-index: 0.9454; 95%CI: 0.9219-0.9689).

The innovation of this paper lies in the construction of an optimal non-linear survival model using a variety of machine learning models, and the demonstration of its superior prognostic performance. While Katzman et al. (2016)[15] proposed a combination of nonlinear and linear models in theory, their prognostic effect lacked empirical research. In contrast, the prognostic performance of the nonlinear proportional hazard survival model developed in this study was significantly improved. From the model correction diagram, the predicted value and the real value are basically in the same straight line, and there is only a small error (Fig. 5). It can also be seen from the forest plot that the higher the TCRS value of the indicator we constructed, the higher the risk of recurrence, and the P value is less than 0.001, indicating that the result is significant (Fig. 7). The constructed risk score index was then used to divide patients into high and low risk groups using X-tile software. The Kaplan-Meier curve showed a significant difference between the two groups, and the log-rank test was less than 0.001, indicating clear differences in survival time and survival rate between the high and low risk groups. Both the training set and the validation set showed that there were significant differences in the high and low analysis groups divided by TCRS (Fig. 6). This predicted non-linear proportional hazard survival model can serve as a quantitative means to assess the high and low risk of atrial fibrillation recurrence in cryoablation patients.

Conclusions

This predicted non-linear proportional hazard survival model can be used as a quantitative means to assess the high and low risk of atrial fibrillation recurrence in cryoablation patients. As survival time increased, the survival rate of patients classified as high risk decreased significantly, while the survival rate of low-risk patients remained at a high level, and the p-value of the log-rank test was less than 0.001.

Study limitations

Some limitations should be considered in our study. First, this study is a retrospective, observational and non-randomized single-center study. Being a retrospective study is a shortcoming in and of itself. Secondly, the training sets and validation sets were from the same medical center, limiting the generalizability of this study's findings. A large-scale multicenter study was also needed to validate the model. Thirdly, although patients who had CIED can appropriately assess the AFLAT recurrence, rhythm follow-up after CBA mainly relies on 24-h Holter ECG, 12-lead ECG, or patient's symptoms.

Declarations

Ethics approval and consent to participate

The purpose along with the methods of this research were fully disclosed to all eligible patients. The subjects granted a written informed consent form. All clinical data is collected in a confidential manner by research members. The study is conducted in accordance with the Helsinki Declaration, the International Conference of Harmonization Good Clinical Practice guidelines, and local regulatory requirements.

Acknowledgements

This study was supported by the Special Projects of the Central Government Guiding Local Science and Technology Development (2021L3018); the Natural Science Foundation of Fujian Province (2021J01658, 2020J01892); the Major Health Research Project of Fujian Province (2021ZD01001). The study also received a research grant from the Natural Science Foundation of Fujian Province (2020J011074) and the Fujian Province Guiding Project for Science and Technology (2018Y0014, 2020Y0062).

Conflicts of Interest: All authors have no conflict of interests.

Authors' Contributions

J.L. and X.W.L. are first co-authors as they have provided equal contributions to this work. J.L., X.P.C. and X.W.L. designed the study. L.C., Y.Z.L., Z.P.Y. and J.Q.C. collected data together. All authors commented on previous versions of the manuscript. All authors had final approval of the submitted and published versions.

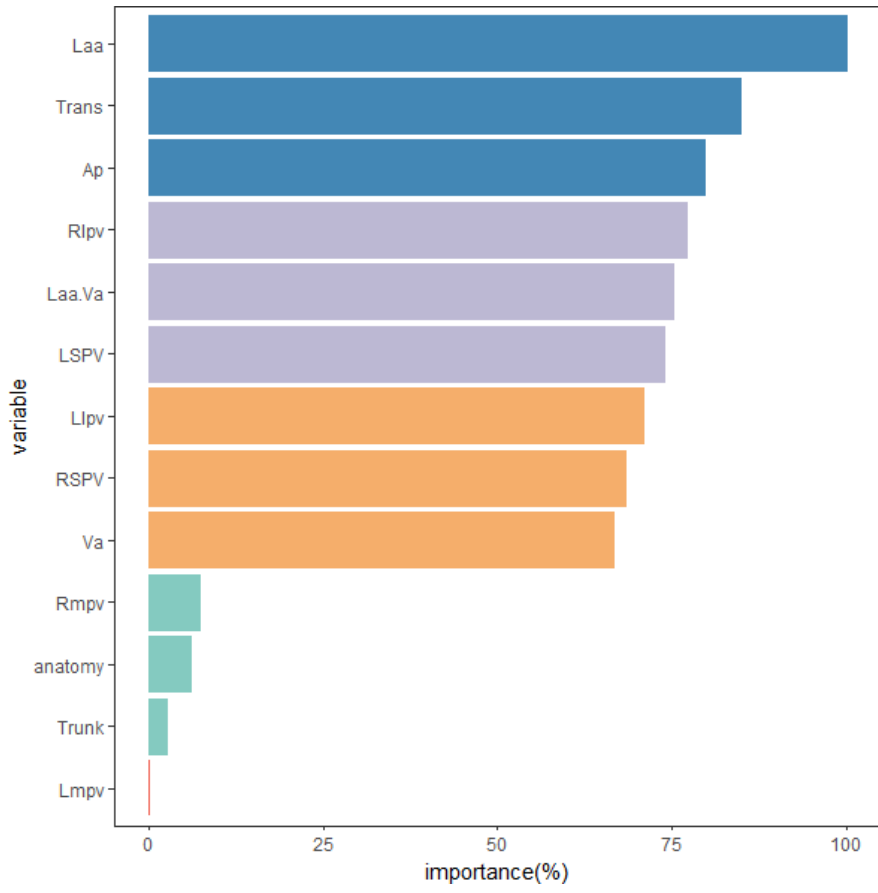
Data availability

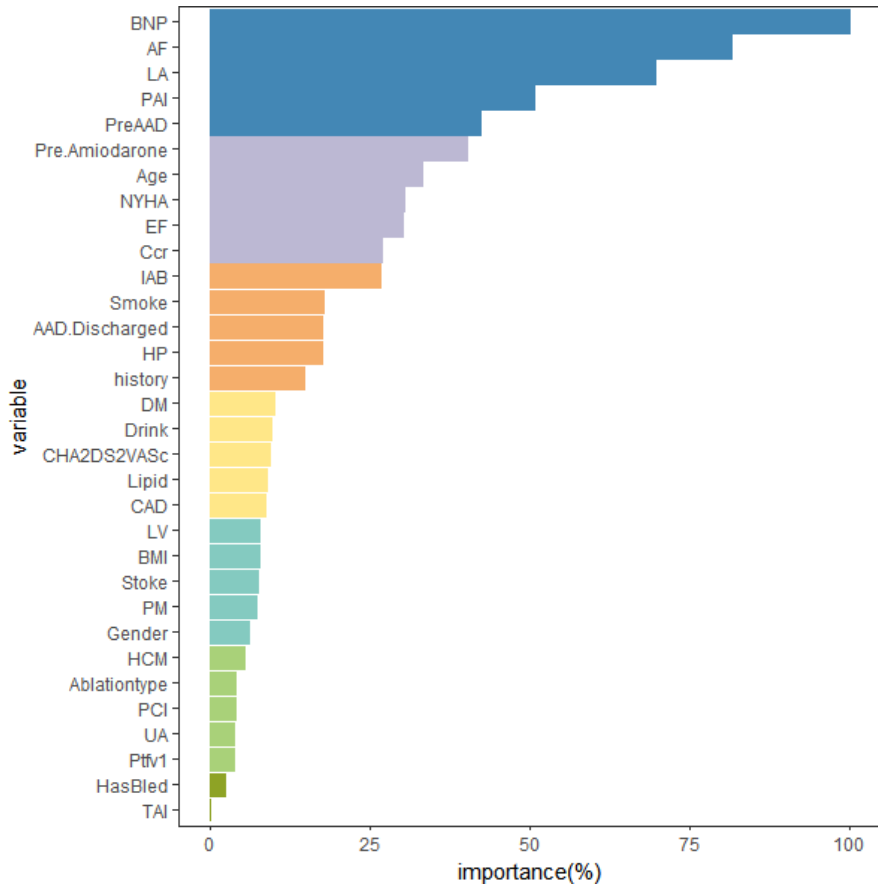
The datasets used and analyzed during the current study available from the corresponding author on reasonable request.

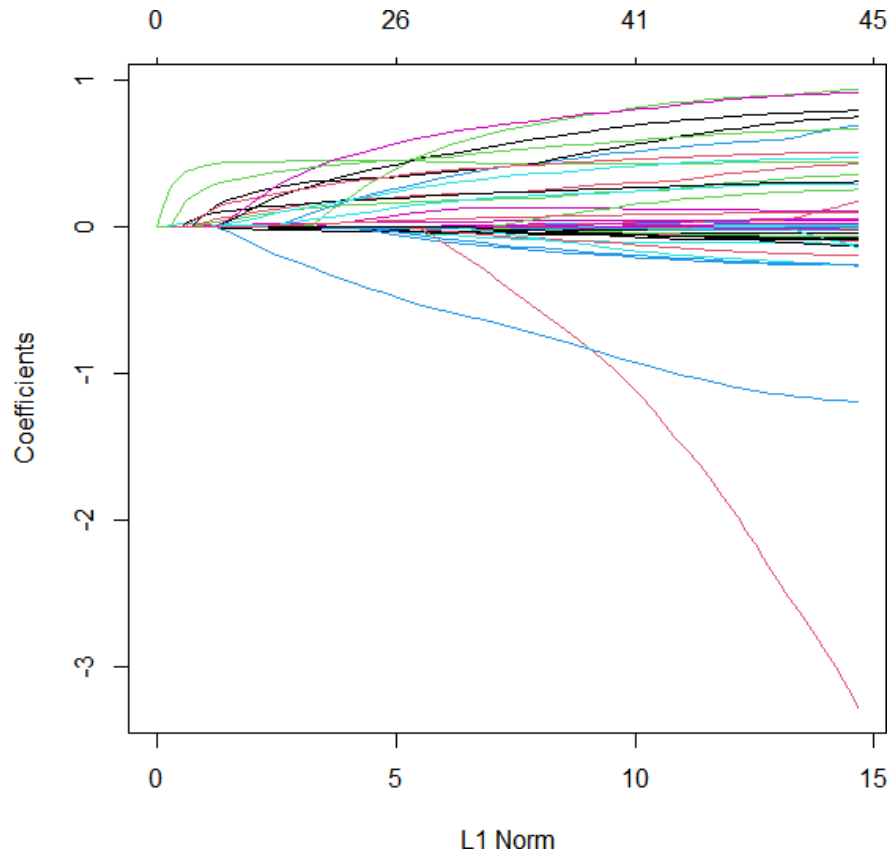
References

1. Kevin SS, Elizabeth PH. Utilizing Biomarkers to Refine Risk Prediction in Atrial Fibrillation. *Journal of the American College of Cardiology* 2019; 73: 1411-1412.
2. Ford GA, Hargroves D, Lowe D, Hicks N, Lip CY, Rooney G, et al. Targeted atrial fibrillation (AF) detection in COVID-19 vaccination clinics. *European Heart Journal. Quality of care & clinical outcomes* 2021; 7: 526-528.
3. Waranugraha Y, Rizal A, Yuniadi Y. A Systematic Review and Meta-Analysis of the Direct Comparison of Second-Generation Cryoballoon Ablation and Contact Force-Sensing Radiofrequency Ablation in Patients with Paroxysmal Atrial Fibrillation. *Journal of Personalized Medicine* 2022; 12: 298-315.
4. Sheng JY, Yang ZN, Xu M, Meng J, Gong MX, Yuxia Miao YX. A prediction model based on functional mitral regurgitation for the recurrence of paroxysmal atrial fibrillation (PAF) after post-circular pulmonary vein radiofrequency ablation (CPVA). *Echocardiography* 2022; 39: 1501-1511.
5. Fürnkranz A, Bordignon S, Dugo D, Perotta L, Gunawardene M, Schulte-hahn B, et al. Improved 1-year clinical success rate of pulmonary vein isolation with the second-generation cryoballoon in patients with paroxysmal atrial fibrillation. *Journal of Cardiovascular Electrophysiology* 2014; 25: 840-844.
6. Aytemir K, Gurses KM, Yalcin MU, Kocyigit D, Dural M, Evranos B, et al. Safety and efficacy outcomes in patients undergoing pulmonary vein isolation with second-generation cryoballoon. *Europace* 2015; 17: 379-387.
7. Greiss H, Berkowitsch A, Wojcik M, Zaltsberg A, Pajitnev D, Deubner N, et al. The impact of left atrial surface area and the second generation cryoballoon on clinical outcome of atrial fibrillation cryoablation. *Pacing and Clinical Electrophysiology* 2015; 38: 815-824.
8. Yalin K, Abdin A, Lyan E, Sawan N, Liosis S, Elsner C, et al. Safety and efficacy of persistent atrial fibrillation ablation using the second-generation cryoballoon. *Clinical Research in Cardiology* 2018; 107: 570-577.
9. Cox DR. Regression models and life-tables. *Journal of the Royal Statistical Society: Series B (Methodological)* 1972; 34: 187-202.
10. Huang JJ, Chen H, Zhang Q, Yang RK, Peng S, Wu ZJ, et al. Development and Validation of a Novel Prognostic Tool to Predict Recurrence of Paroxysmal Atrial Fibrillation after the First-Time Catheter

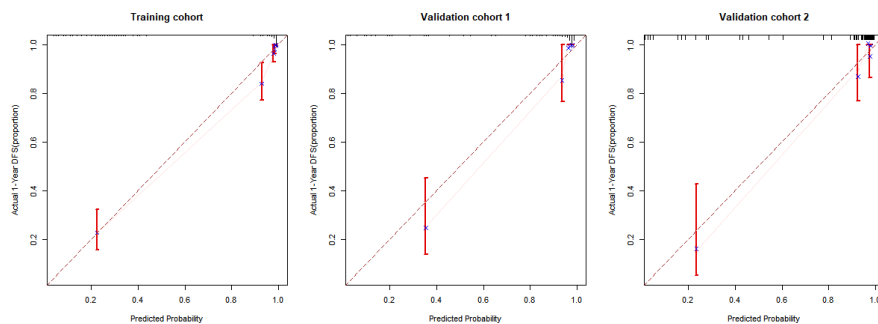
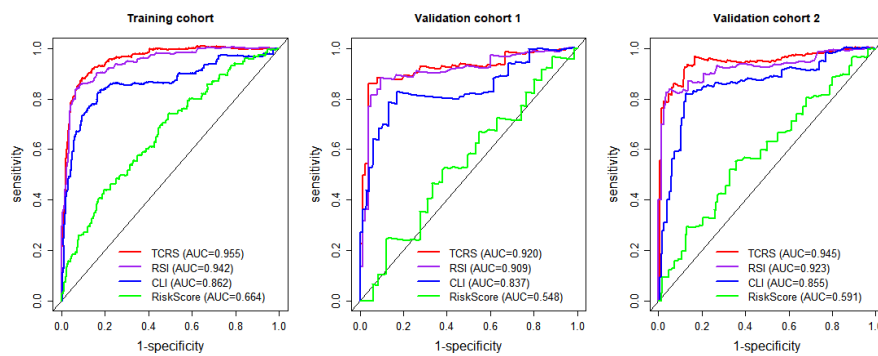
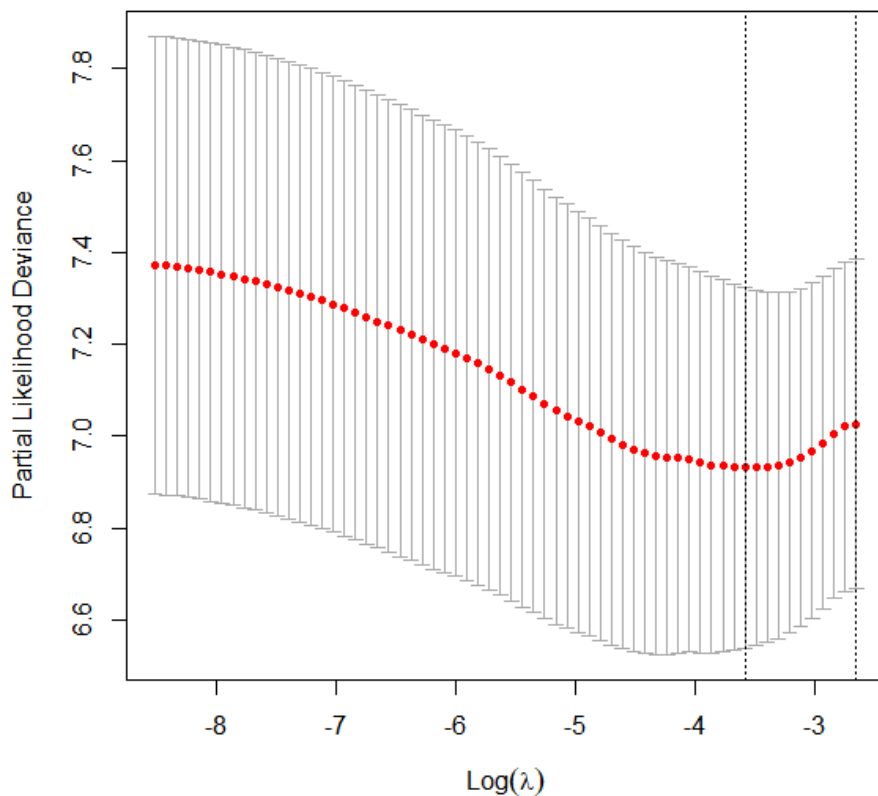
- Ablation: A Retrospective Cohort Study. *Diagnostics* 2023; 13: 1207-1221.
11. Pramod A, Naicker HS, Tyagi AK. Machine learning and deep learning: Open issues and future research directions for the next 10 years. *Computational analysis and deep learning for medical care: Principles, methods, and applications* 2021: 463-490.
 12. Li L, Tu B, Xiong Y, Hu Z, Zhang ZH, Liu SY, et al. Machine Learning-Based Model for Predicting Prolonged Mechanical Ventilation in Patients with Congestive Heart Failure. *Cardiovascular Drugs and Therapy* 2022: 1-11.
 13. Jiang Y, Xie J, Han Z, Liu W, Xi SJ, Huang L, et al. Immunomarker Support Vector Machine Classifier for Prediction of Gastric Cancer Survival and Adjuvant Chemotherapeutic Benefit Immunomarker SVM-Based Predictive Classifier. *Clinical Cancer Research* 2018; 24: 5574-5584.
 14. Utkin LV, Satyukov ED, Konstantinov AV. SurvNAM: The machine learning survival model explanation. *Neural Networks* 2022; 147: 81-102.
 15. Katzman JL, Shaham U, Cloninger A, Bates J, Jiang TT, Kluger Y. Deep survival: a deep cox proportional hazards network. *stat 1050. IEICE Transactions on Fundamentals of Electronics, Communications and Computer Sciences*, 2016: 1-10.
 16. Faraggi D, Simon R. A neural network model for survival data. *Statistics in Medicine* 1995; 14: 73-82.
 17. Wyndham C. Atrial fibrillation: the most common arrhythmia. *Texas Heart Institute Journal* 2000; 27: 257-267.
 18. Yao MH, Ren CL, Zhang L, Li LG, Jiang SL. Short-term and mid-term effects of radiofrequency ablation in mitral valve surgery in patients with different left atrial sizes. *Journal of Thoracic Disease* 2020; 12: 6030-6068.
 19. Liu J, Kaufmann J, Kriatselis C, Fleck E, Gerds-Li JH. Second generation of cryoballoons can improve efficiency of cryoablation for atrial fibrillation. *Pacing and Clinical Electrophysiology* 2015; 38: 129-135.
 20. Meyre P. Incidence of and causes for all-cause hospitalizations in patients with atrial fibrillation. University of Basel 2019.
 21. Peng H, Dong D, Fang MJ, Li L, Tang LL, Chen L, et al. Prognostic value of deep learning PET/CT-based radiomics: potential role for future individual induction chemotherapy in advanced nasopharyngeal carcinoma. *Clinical Cancer Research* 2019; 25: 4271-4279.
 22. Bieging ET, Morris A, Wilson BD, McGann CJ, Marrouche NF, Cates J. Left atrial shape predicts recurrence after atrial fibrillation catheter ablation. *Journal of cardiovascular electrophysiology* 2018; 29: 966-972.
 23. Zhou XJ, Zhang LX, Xu J, Zhu HJ, Chen X, Wang XQ, et al. Establishment and evaluation of a nomogram prediction model for recurrence risk of atrial fibrillation patients after radiofrequency ablation. *American Journal of Translational Research* 2021; 13: 10641.
 24. Dong Y, Zhai Z, Zhu B, Xiao SC, Chen Y, Hou AX, et al. Development and validation of a novel prognostic model predicting the atrial fibrillation recurrence risk for persistent atrial fibrillation patients treated with nifekalant during the first radiofrequency catheter ablation. *Cardiovascular Drugs and Therapy* 2022: 1-13.
 25. Hill NR, Ayoubkhani D, McEwan P, Sugrue DM, Farooqui U, Lister S, et al. Predicting atrial fibrillation in primary care using machine learning. *PloS one* 2019; 14: e0224582.
 26. Betancur J, Otaki Y, Motwani M, Lemley M, Dey D, Gransar H, et al. Prognostic value of combined clinical and myocardial perfusion imaging data using machine learning. *JACC: Cardiovascular Imaging* 2018; 11: 1000-1009.
 27. Chen YH, Lu ZY, Xiang Y, Hou JW, Wang Q, Lin H, et al. Cryoablation vs. radiofrequency ablation for treatment of paroxysmal atrial fibrillation: a systematic review and meta-analysis. *Europace* 2017; 19: 784-794.
 28. Wang XH, Li Z, Mao JL, Zang MH, Pu J. Low voltage areas in paroxysmal atrial fibrillation: The prevalence, risk factors and impact on the effectiveness of catheter ablation. *International Journal of Cardiology* 2018; 269: 139-144.
 29. Penela D, Cappato R. How effective is cryoablation in the treatment of atrial fibrillation?. *European Heart Journal Supplements* 2021; 23: 51-54.

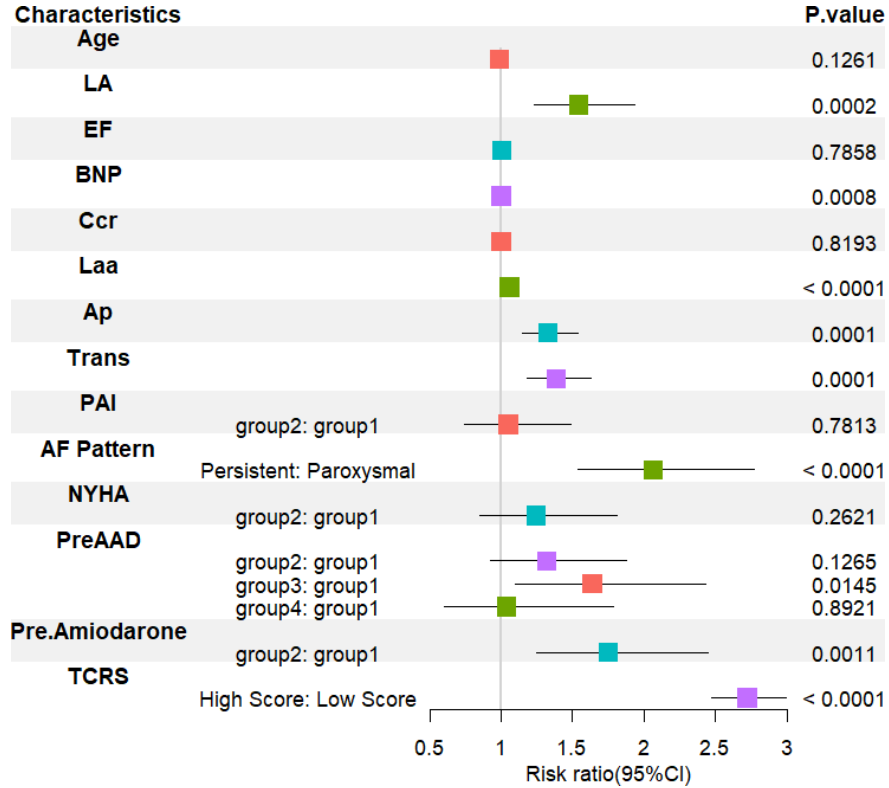
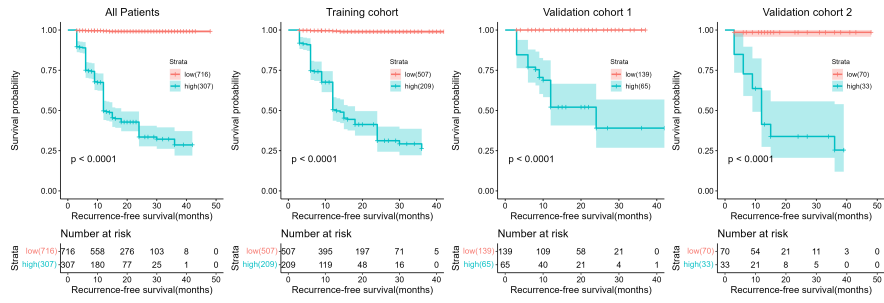






45 45 44 43 43 41 39 32 26 20 10 4 2 1





Hosted file

Table.docx available at <https://authorea.com/users/666743/articles/667471-improved-prognostic-value-of-recurrence-for-atrial-fibrillation-patients-after-cryoablation-by-non-linear-survival-models>